HUNTINGTON MEDICAL RESEARCH INSTITUTES
NEUROLOGICAL RESEARCH LABORATORY
734 Fairmount Avenue
Pasadena. California 91105

Contract No. NO-NS-82388

QUARTERLY PROGRESS REPORT
April 1 - June 30. 1999

Report No. 6

"SAFE AND EFFECTIVE STIMULATION OF NEURAL TISSUE"

William F. Agnew, Ph.D.
Ted G.H. Yuen, Ph.D.
Douglas B. McCreery. Ph.D.
Leo Bullara, B.A.

ABSTRACT

In the last quarter, we have continued our evaluation of intracortical microstimulation of the cat's cortex. In the most recent study, we have investigated the etiology of persistent, randomly distributed gliosis along the shafts of Epoxylite-coated microelectrodes. A biocompatibility study was carried out in which various microelectrode insulators and fabrication techniques were evaluated to attempt to determine the origin of the gliosis. The results taken from multiple implants in 3 animals failed to implicate a specific electrode insulation or other materials since gliosis was present adjacent to microelectrodes regardless of their insulation or treatment during fabrication. These results suggest that the source of the gliosis is a contaminant reaching the electrodes by aerosols or particulate matter.

INTRODUCTION

Over the last year we have frequently reported the presence of gliosis, with or without lymphocytes, randomly distributed along the shafts of Epoxylite-coated iridium microelectrodes (QPR's 2 and 4, 1998). This reaction had been observed adjacent to both pulsed and unpulsed microelectrodes. In this quarter we focused on the incidence and pattern of distribution around multiple implants of unpulsed iridium electrodes coated with Masterbond epoxy, Epoxylite, Parylene and silicon carbide. Coating of microelectrodes with Parylene was carried out at Bioelectric Corp., courtesy of Dr. Lou Rucker, and silicon carbide microelectrodes were coated at EIC courtesy of Dr. Stuart Cogan

METHODS

Microelectrode implants. Table 1 presents the three animal experiments in which the components used in fabrication procedures and 3 microelectrode insulators were evaluated by implantation of microelectrodes in the cruciate and/or parietal cortices for a period of 30 days. In IC-181, uncoated iridium microelectrode shafts, and also iridium shafts coated with Masterbond (both with a Masterbond ball at the top of

the shaft), were implanted. In IC-183, the microelectrodes were coated with Epoxylite with an Epoxylite ball at the top of the shaft. In IC-187, three microelectrode insulators (Epoxylite. Parylene and silicon carbide) were evaluated for gliotic reactions and other aspects of biocompatibility. All of the implants were passive (unstimulated). We also evaluated the possibility of oil vapors from a vacuum pump used in curing of insulators, as a possible cause of gliosis.

Surgical technique. Using general anesthesia and using aseptic techniques, the skin and muscles were reflected in a midline incision, and the cruciate or parietal cortex exposed in a craniectomy. The frontal air sinus was cleaned and filled with cranioplasty. The implants were then made manually (single electrodes) using a forceps to grasp the epoxy or Masterbond ball at the top of the electrode, or using a vacuum-electrode holder attached to a stereotaxic carrier. The dura was not sutured; rather, the electrodes were covered with a 1 × 1 cm piece of fascia removed from the right temporalis muscle. Bacitracin was added to the wounds and the muscle and dermis closed in layers. The locations of the various implants are given in Table 1.

Histology. At one month after the implantation, the cats were anesthetized with Nembutal and perfused through the ascending aorta with ½-strength Karnovsky's fixative. Blocks of tissue containing one or more electrode sites were cut to enable horizontal serial sectioning after paraffin embedment.

Histologic evaluations were carried out on serial 8 μm thick paraffin sections cut in the horizontal plane (perpendicular to the electrode shafts). The sections included both single and multiple microelectrode implants on the cruciate or parietal gyri. Serial sections enabled observation of histologic alterations along the entire shaft. At 100 μm intervals below the pial surface, we recorded the presence of any inflammatory cells, hemorrhage, cavitation, scarring, gliosis, edema, sheath thickness, as well as the condition of the neurons and the appearance of blood vessels in the area at these levels. Criteria for quantitation (+ to +++) for gliosis and microhemorrhages are given in Table 1.

TABLE 1
IC 181, 183, 187
(BIOCOMPATIBILITY SERIES)
HISTOLOGY REPORT

C	IMPLANT MATERIA	ELECTRODE NO	LOCATION (GYRUS)		DURATION OF IMPLANT	GLIOSIS (ESTIMATES)	NEURONS	SCARS
181	Masterbond Ball & Masterbond Coated Iridium Shaft	141	L Posterior		1 month	+ to +++	N	S
	Masterbond Ball & Masterbond Coated Iridium Shaft	142	L Posterior			Rare	N	+ M
	Masterbond Ball & Masterbond Coated Iridium Shaft	143	L Posterior			0 to + -	N	C
	Masterbond Ball & Masterbond Coated Iridium Shaft	144	L Posterior			0 to ++	Occas Flat	+ M
	Masterbond Ball & Shaft (uncoated)	145	L Precruc			+ to +++	Indistinct ; Smudgy ; at ~700 µm depth	0
	Masterbond Ball & Shaft (uncoated)	146	L Precruc			0 to +	N	S
	Masterbond Ball & Shaft (uncoated)	147	L Precruc			0 to +	N	+ M
183	Epoxylite Ball Epoxylite-Coated Shaft (Vacuum)	149	L Marginalis		1 month	0 to +++	Occas Shrunken	0
	Epoxylite Ball Epoxylite-Coated Shaft (Vacuum)	152	L Marginalis			0 to +	Occas Flat A Few Stellate	+ M
	Epoxylite Ball Epoxylite-Coated Shaft (No Vacuum)	153	L Suprasylvius			0	Occas Flat	+ M
	Epoxylite Ball Epoxylite-Coated Shaft (No Vacuum)	154	L Suprasylvius			0 to +	Occas Flat	+ M
	Epoxylite Ball Epoxylite-Coated Shaft (No Vacuum)	155	L Suprasylvius			0 to +	N	+ M
	Epoxylite Ball Epoxylite-Coated Shaft (No Vacuum)	156	L Suprasylvius			0 to +	Occas Flat	+ M
18	Silicon Carbide-Coated Shaft	11	L Supra sylvius	Ant Array	1 month	0 to ++	Occas Flat	0
	Silicon Carbide-Coated Shaft	15	L Supra-sylvius	Ant Array		0 to ++	Occas to Several Flat	+- H
	Silicon Carbide-Coated Shaft	11	L Supra-sylvius	Post Array		0 to +++	A Few Flat A Few Smudgy	+ H
	Silicon Carbide-Coated Shaft	15	L Supra-sylvius	Post. Array		0 to +++	Occas Flat	++ H
	Epoxylite-Coated Shaft	17	L Supra-sylvius	Ant Array		Occas to +++	Occas Flat	++ H
	Epoxylite-Coated Shaft	19	L Supra-sylvius	Ant Array		0 to ++	Occas Flat	++ H
	Epoxylite-Coated Shaft	17	L Supra-sylvius	Post Array		0 to +++	Occas Flat	++ H
	Epoxylite-Coated Shaft	19	L Supra-sylvius	Post Array		0 to +++	Occas Flat	++ M
	Parylene-Coated Shaft	14	L Supra-sylvius	Ant Array		+ to ++	Occas Flat	++ H
	Parylene-Coated Shaft	9	L Supra sylvius	Ant Array		+ to ++	Occas Flat	+ H
	Parylene-Coated Shaft	14	L Supra-sylvius	Post Array		+ to ++-	Occas Flat	++ H
	Parylene-Coated Shaft	9	L Supra-sylvius	Post Array		0 to +	Occas Flat	S
	Uncoated Ir Shaft	10	Ant Array			0 to +++	Occas Flat	+++, H,M
	Uncoated Ir Shaft	10	Post Array			0 to +--	Occas Flat	++ H

- = Slight (estimated 0-49 cells)
++ = Moderate (estimated 50-99 cells)
+++ = Marked (estimated 100+ cells)

H = Hemorrhagic Etiology (circumferential scar)
M = Movement Etiology (directional scar)

N = Normal

RESULTS

The results are summarized in Table 1. Two types of scarring were observed near the electrode tracks. In Animals IC-181 and IC-183, both types of scars were probably due to a mechanical etiology, i.e., vascular disruption (microhemorrhage) or directional scars due to trauma during insertion or later movement. Generally, the latter were narrow and linear, reaching a maximum length of 500 μm. In IC-187, the scars, probably due to resolution of hemorrhage, were almost always rounded and circumferentially distributed and surrounded the tracks. Most of these fibroglial scars attained diameters of 130 to 450 μm.

A. **Animal No. IC-181.**

1. Masterbond Ball and Uncoated Iridium Shaft. Along one of the three electrodes, neurons appeared ill-defined and "smudgy." This track was also accompanied by gliosis ranging from zero to +++ (Fig. 1A&B: see Table 1 for quantitative criteria). The remaining two tracks showed normal neurons no greater than + gliosis. One of the electrodes was accompanied by a linear scar which we presume is due to electrode movement.

2. Masterbond Ball and Masterbonded-Coated Ir Shaft. Four individual electrodes were inserted into the left postcruciate gyrus. Aside from occasional flat neurons near one of the electrodes, all neurons appeared normal. Linear scars accompanied two tracks, indicating electrode movement. At various depths below the pia, gliosis was rare along one electrode track, ranged from zero to ++ near two others and from + to +++ at the remaining track (Fig. 2A&B).

B. **Animal No. IC-183.**

1. Epoxylite Ball and Epoxylite-Coated Ir shafts without vacuum pump exposure. Four electrode tracks (#'s 153-156) were present in the left gyrus suprasylvius. Neurons near one track were normal and occasional flat neurons were present near the remaining three tracks. Gliosis was either absent or no more than + at three tracks and absent at the fourth track. Linear (movement-caused) scars were present at all tracks.

2. Epoxylite Ball and Epoxylite-Coated Ir shaft with vacuum pump exposure. Two of four tracks were found on the left gyrus marginalis (#'s 149 and 152). One track was accompanied by occasional shrunken neurons and gliosis ranging from zero to +++. The remaining track showed little or no gliosis and a few flattened neurons along with occasional stellate neurons. A linear scar was present at one track.

C. **Animal No. IC-187.** Two seven-shaft arrays were implanted into the left gyrus suprasylvius. One of the tracks in each array was left by an uncoated Ir stabilizer shaft. Each array contained two electrodes coated with silicon nitride, Epoxylite or Parylene. The findings will be described by combining all implants having the same type of polymer coating.

1. Uncoated Ir Stabilizer Tracks. For the most part, neurons along both tracks appeared normal but occasional flat neurons frequently were found. Both tracks were accompanied by a rounded scar, and one of these also contained a linear scar, signifying electrode movement as well as a hemorrhagic etiology. Both tracks were accompanied by a wide range of gliosis ranging from none, highly localized (Fig. 3A) to +++, and completely surrounding the track (Fig. 3B).

2. Silicon Carbide Coated Shafts. Aside from a few ill-defined ("smudgy"-appearing) neurons, all neurons appeared either normal or somewhat flattened. Three of the four tracks were accompanied by small scars which appeared to be the sequela of a previous small hemorrhage which had resolved into a compact scar, rather than the result of electrode movement (Fig. 4A). Gliosis at or near the track ranged from none to +++ (Fig. 4B). In actuality, two of the four tracks in this group were accompanied by the +++ gliosis.

3. Epoxylite Coated Shafts. There were occasional flattened neurons near all tracks but the greatest majority appeared normal. All tracks were accompanied by a small scar, probably the result of a small hemorrhage. In addition, one of these also contained a short linear component, presumably caused by electrode movement. Gliosis ranged from none up

to ++ (Fig. 5A) at one track but up to +++ at the remaining three tracks (Fig. 5B).

4. Parylene Coated Shafts. Three of four tracks were accompanied by well-developed, rounded fibroglial scars, probably of hemorrhagic etiology. The remaining track showed no scar. Along one track, gliosis was mild (0 to +), moderate at one track (+ to ++) and marked along the two remaining tracks (+ to +++) (Fig. 6A&B).

Gliosis. The distribution of gliosis along the several electrode and stabilizer tracks varied widely with respect to the amount of gliosis along individual tracks or those left by electrodes having the same type of polymer coating and even around those from uncoated iridium stabilizer shafts Fig. 7A shows a horizontal section through all 7 tracks of the anterior array at a depth of 500 µm below the pia. Here, there is little or no gliotic accumulation at any track. However, random accumulations of glia varied in numbers of accumulated astrocytes at other levels. Fig. 7B shows that at a depth of 200 µm below the pia, all tracks of the posterior array except numbers #9 (Parylene) and #10 (stabilizer) are accompanied by moderate to marked gliosis. As mentioned above, varying amounts of gliosis, (or none) skirted the tracks at other levels.

Microhemorrhage and scarring. Table 1, last column, presents the incidence of scars due either to healed microhemorrhages or to mechanical movement of the electrodes. In Animals IC-181 and IC-183, the electrodes were single and inserted manually with a forceps: there were no resolved microhemorrhages along the tracks or at the tips of the electrodes. However, 8 tracks showed movement (directional) scars, primarily at or near the tip. These scars were probably healed slashes occurring during implantation, but we cannot rule out movement of the electrodes after implantation.

In Animal IC-187, two 7-electrode (1 stabilizer) arrays were inserted fairly slowly (approximately 2 seconds) using a vacuum-array holder mounted on a stereotaxic carrier. Of the 14 electrode sites, 12 had + to +++ microhemorrhages; however, directional scars were present in only 2 of the 14.

DISCUSSION

Several conclusions may be drawn from these results. First, gliosis was randomly distributed (or absent entirely) adjacent to the electrode tracks coated with four different materials (Masterbond, Epoxylite, Parylene and silicon carbide) and also uninsulated iridium shafts. If the source was some type of toxic substance chronically emanating from the insulators, it would be expected that this would occur on all electrodes along their entire length. The fact that the three insulators were applied to the microelectrodes in 3 different laboratories, using different techniques, suggests that the gliosis may be due to a contaminant adhering to the electrodes during some step in assembly or surgical procedure at HMRI. In addition, gliosis was also observed adjacent to uninsulated iridium shafts. One suspect material was oil vapor from the pump used to evacuate the air from the curing oven. One of two Epoxylite-coated electrodes cured under these conditions, resulted in one electrode with +++ gliosis. However, other electrodes, some insulated in other laboratories, were 0 - +++ with or without vacuum pump exposure. This finding virtually eliminates pump oil vapors as a source of the gliosis.

Rousche and Normann (1998) reported on intracortical implants of silicon microelectrodes insulated with polyimide. After six-month implantations, histologic studies showed a chronic astroglial reaction quite similar to that observed in this study. The authors had no explanation for the apparently random occurrence of the gliosis. Thus, their report represents a fifth insulating material to be accompanied by a gliotic reaction. This supports our assumption that the gliosis is unrelated to the insulating material. These findings, taken together, emphasize the extreme sensitivity of the cortical microenvironment to as yet unidentified material(s) present on insulated or uninsulated iridium shafts.

It is noteworthy that the distribution of the gliosis is sometimes highly localized on one side of the electrode track and sometimes takes the form of several layers of cells completely surrounding the track. This suggests the possibilities that the contaminants are aerosols taken up during processing or particulate matter adherent to the electrodes by static charge. It should be noted in the micrographs that the neuronal loss or displacement by the gliotic mass was appreciable and extended up to 350 μm from the electrode track. It is of significance that a fibroglial sheath was entirely absent

(one month after implantation) in the gliotic sites adjacent to electrode tracks. This indicates an ongoing toxic reaction (compare the thin sheath of Fig. 5B with Figs. 1, 2. 3, 4, 5A and 6). We consider this toxicity to be a serious problem and have suspended our cortical microstimulation protocols to resolve the etiology. In future experiments we will sonicate the electrode arrays in alcohol after unpackaging in the surgical suite. followed by an alcohol flush just prior to implantation. We will also further investigate each step of the fabrication procedures. We will also use a clean room for the final stages of fabrication and, finally. our surgical suite is being equipped with a pre-filter, hepa filter at the air intake and a 4" fan at the return vent.

Microhemorrhages. Resolved microhemorrhages were completely absent adjacent to manually inserted electrodes (IC-181 and IC-183); however, with 7-electrode arrays inserted stereotaxically. 12 of 14 tracks were accompanied by generally small resolved microhemorrhages (i.e.. scars). This marked difference with different insertion techniques is not understood but indicates the importance of continuing investigation of the mode and insertion velocity of microelectrodes.

REFERENCE

Rousche. P.J. and Normann. R.A.: Chronic recording capability of the Utah intracortical electrode array in cat sensory cortex. J. Neuroscience Methods, 82:1-15, 1998.

WORK NEXT QUARTER

We will continue our investigation of the etiology of the gliosis by implementing the measures suggested in the Discussion section as well as a step-by-step evaluation of our electrode handling procedures, including fabrication steps, cleaning protocol and surgical implantation.

Fig. 1. A. Animal IC-181. Track #14, Masterbond ball and uncoated iridium shaft. Depth = 900 µm. Approximately 12 layers of glial cells surround the track (T). A few lymphocytes (arrows) are admixed with the glial cells. Note the lymphocyte cuffing around a nearby blood vessel (V). This and all subsequent micrographs are from 8 µm thick paraffin sections. There is a conspicuous lack of a fibroglial sheath around the track. Neurons were normal-appearing but the closest to the track were 130 µm. Nissl stain. Bar = 50 µm. **B.** Same track as shown in A above. Depth = 1,100 µm. Numerous glial cells and several lymphocytes (arrows) surround the track (T) in an asymmetrical pattern. Nearby blood vessels (V) are cuffed with lymphocytes. Nissl stain. Bar = 100 µm.

Fig. 2. A. Animal IC-181. Electrode track #142. Masterbond bail and Masterbond coated iridium shaft, left postcruciate gyrus. Depth = 400 µm. The track (T) is surrounded asymmetrically by numerous glial cells and lymphocytes. A slight tear communicates with the lumen of the track. This probably occurred during electrode removal. Vascular hyperplasia is prominent (V). At greater magnification, the neurons appeared normal; however, the closest neurons were 50 µm or more from the track. As in Fig. 1, the sheath is not present. Nissl stain. Bar = 100 µm.
B. Tip (T) of track shown in **A** above. A directional scar. The comet-like appearance of the track with "streaming" connective tissue indicates movement of the electrode during or after insertion. Several glial cells are incorporated into the partially formed connective tissue scar (delimited by the arrows). Vascular hyperplasia (V) is present. Nissl stain. Bar = 50 µm.

Fig. 3. A. Animal IC-187. Uncoated iridium stabilizer track (#10), posterior array left gyrus suprasylvius. Depth = 305 µm. Aside from a small focus of glial cells (arrows), the track (T) is skirted by a markedly thin sheath. A few neurons (arrow heads) near the track are flattened although the remaining neurons in the field appear normal. Nissl stain. Bar = 50 µm.
B. Same track as in **A** above at a depth of 500 µm. Several layers of glial cells symmetrically surround the track (T). One nearby blood vessel (V) is cuffed with lymphocytes. Nearby neurons appear normal. Nissl stain. Bar = 50 µm. All subsequent micrographs are also from Animal IC-187.

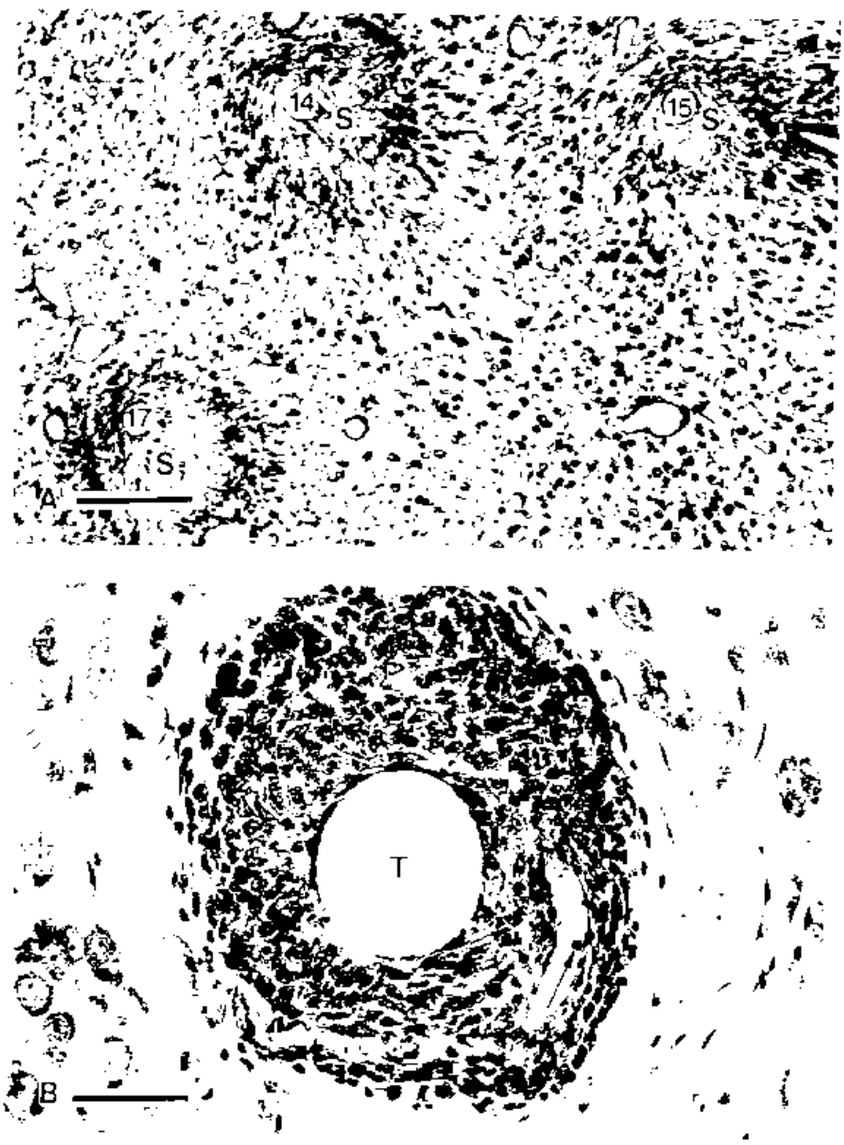

Fig. 4. **A.** Anterior array site, left gyrus suprasylvius. Electrode tracks #17, #14 and #15 are marked and represent tracks left by iridium shafts coated with Epoxylite, Parylene and silicon carbide respectively. Depth = 700 µm. The tracks are surrounded by well-developed scars (S) measuring about 235 to 290 µm in diameter. Their rounded shapes favor a resolved hemorrhage rather than the more typical narrow, highly directional scar left by a misaligned or migrating electrode. Nissl stain. Bar = 200 µm.
B. Same track (#15, silicon carbide) as that seen in **A** above. Depth = 100 µm. Approximately ten glial cell layers surround the track (T). A solitary lymphocyte (arrow) is present in a blood vessel surrounded by glia. Lymphocytes are also present along the right border of this accumulation of glial cells. Nissl stain. Bar = 50 µm

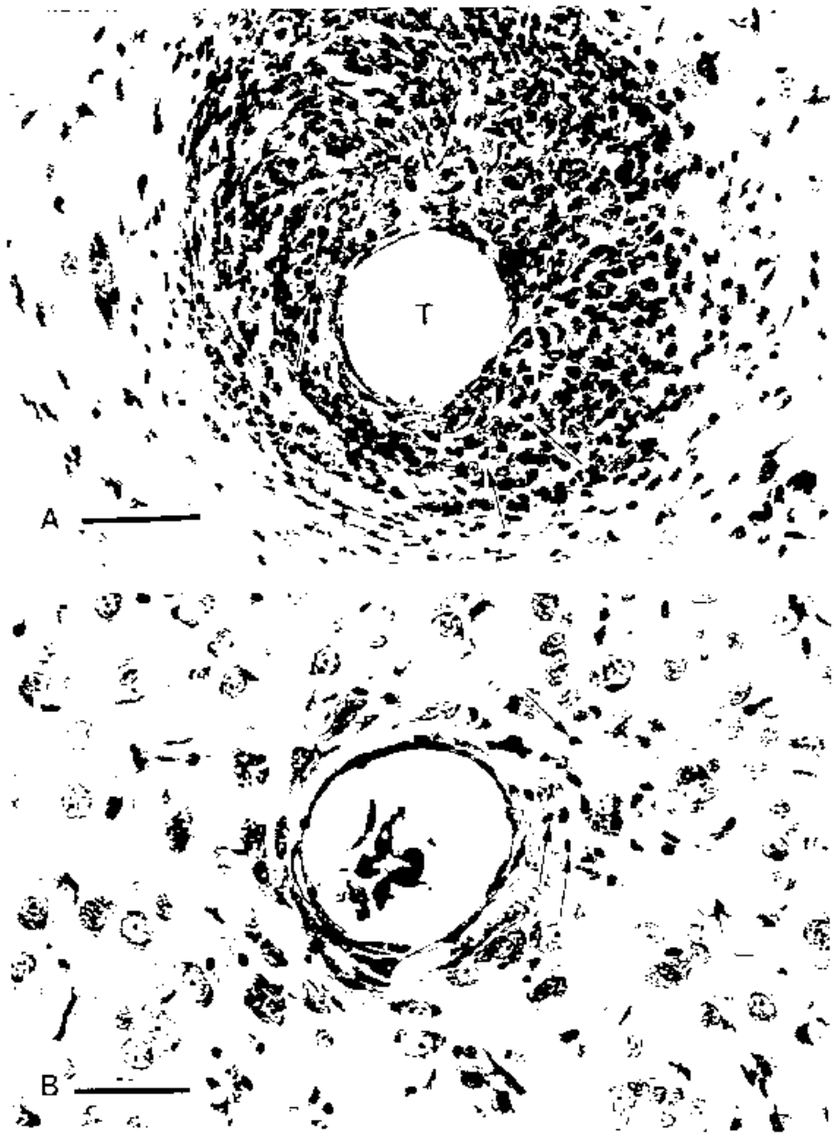

Fig. 5. A. Track #17 (Epoxylite), posterior array. At the electrode entry site, the track (T) is surrounded by numerous glia and several lymphocytes (arrows) but lacks a well-formed sheath. Occasional nearby neurons were somewhat flattened. Nissl stain. Bar = 50 µm.

B. Same track as in A above. Depth = 300 µm. Aside from a few loosely scattered glia (arrows) the track is virtually free of a glial response. The sheath is thin and nearby neurons are only slightly flattened. Nissl stain. Bar = 50 µm.

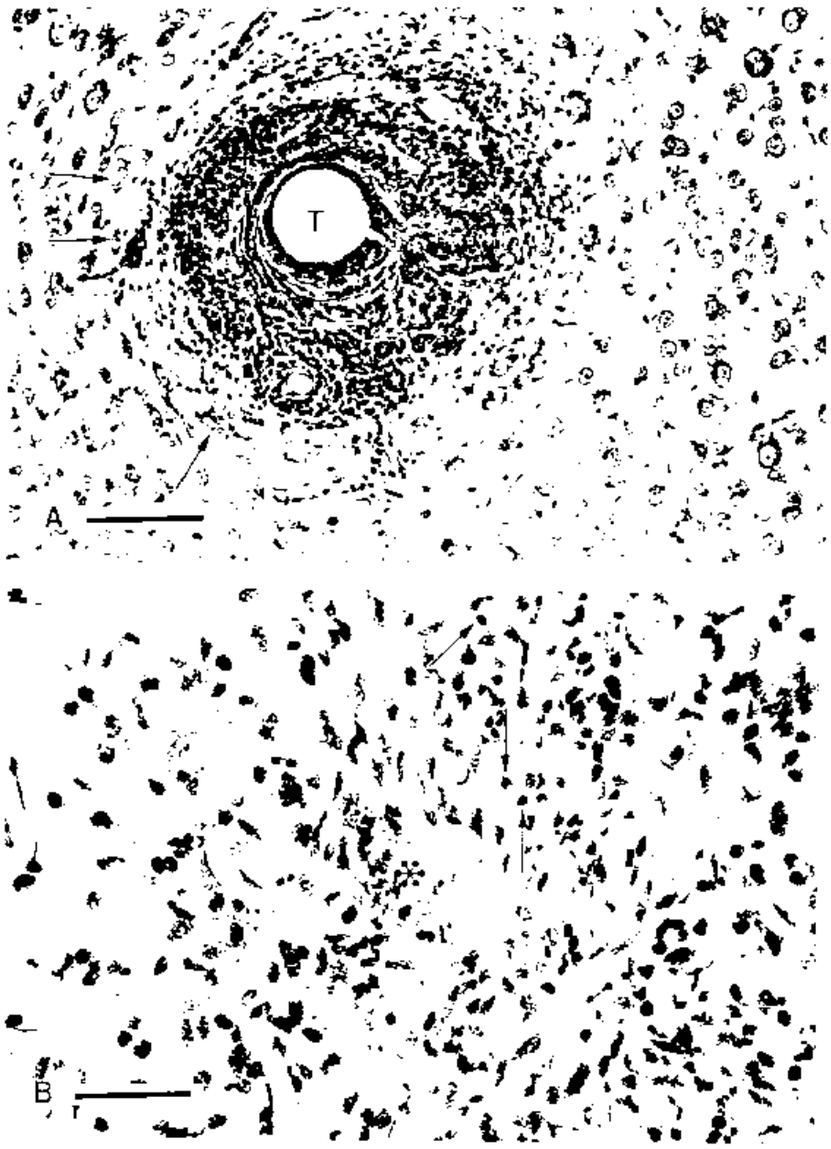

Fig. 6. **A.** Track #14 (Parylene) in posterior array. Depth = 300 µm. Numerous lymphocytes (small, dark round cells) surround the glial aggregate around the track (T). Aside from a few flattened neurons (arrows), most neurons appear normal. Nissl stain. Bar = 100 µm. **B.** Tip site (asterisk) of same track #14 as shown in **A** above. Numerous, loosely dispersed astrocytes (arrows) are scattered near the tip. The neuropil appears normal. H&E stain. Bar = 50 µm.

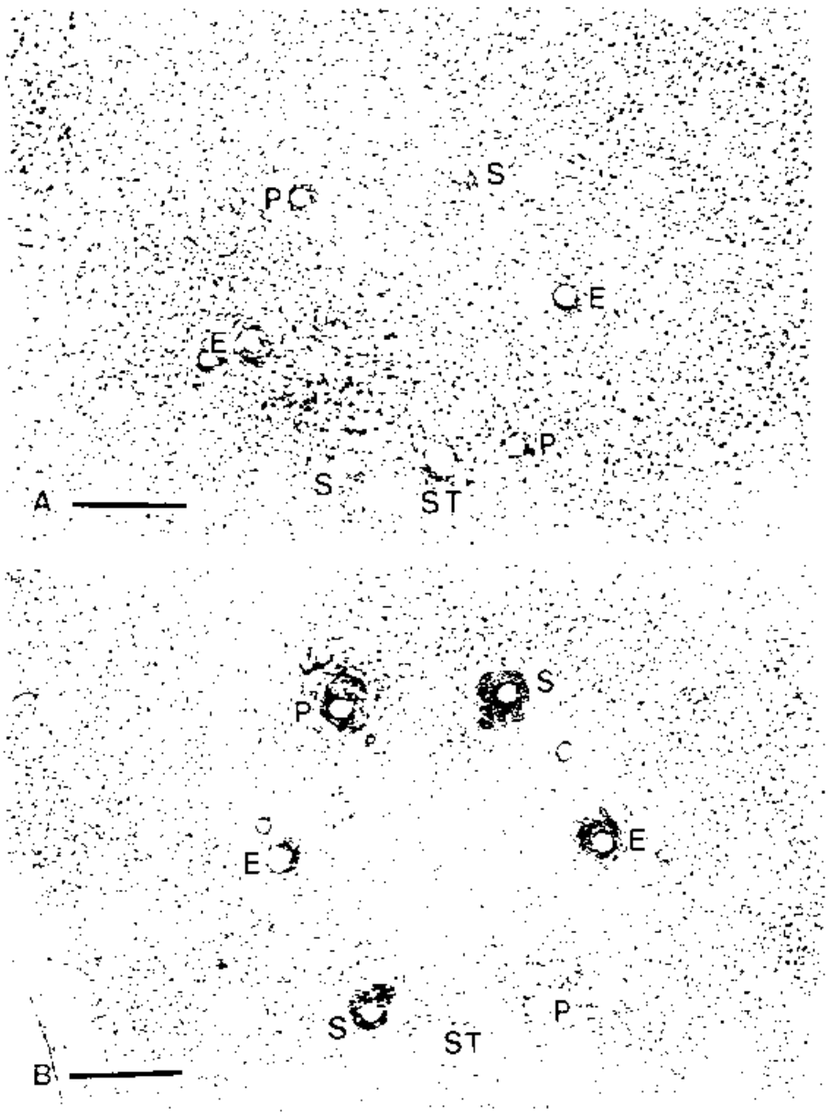

Fig. 7. A&B. Anterior and posterior array sites, respectively. Depths of the anterior and posterior array sites are 500 and 200 µm, respectively. The two micrographs are compared to demonstrate that the host response varied widely in the presence of identical type polymers. For example, note the gliosis or virtual lack of it, around silicon carbide tracks (S) in the two array sites. The same applies to the Parylene (P) and Epoxylite sites (E). ST = stabilizer tracks. Both sections are stained with H&E. Each bar = 500 µm.